A new genome allows the identification of genes associated with natural variation in aluminium tolerance in *Brachiaria* grasses

Margaret Worthington[1#], Juan Guillermo Perez[1], Saule Mussurova[2], Alexander Silva-Cordoba[1], Valheria Castiblanco[1], Charlotte Jones[3], Narcis Fernandez-Fuentes[3], Leif Skot[3], Sarah Dyer[2&], Joe Tohme[1], Federica Di Palma[2], Jacobo Arango[1], Ian Armstead[3], Jose J De Vega[2*]

1. International Center for Tropical Agriculture (CIAT), A.A. 6713, Cali, Colombia.
2. Earlham Institute, Norwich Research Park, Norwich, NR4 7UZ, UK.
3. Institute of Biological, Environmental and Rural Sciences (IBERS), Aberystwyth University, Aberystwyth, UK.

Present address: Department of Horticulture, University of Arkansas, 306 Plant Sciences Bldg, Fayetteville, AR, 72701, USA.
& Present address: NIAB, Huntingdon Road, Cambridge, CB3 0LE, UK.

* Correspondence to jose.devega@earlham.ac.uk; Earlham Institute, Norwich Research Park, Norwich, NR4 7UZ, UK.

Running title: Genetic control of aluminium tolerance in *Brachiaria.*

6,494 words.

HIGHLIGHT

We identified QTLs, genes and molecular responses in high and low tolerant *Brachiaria* grasses associated with aspects of response to aluminium stress, such as regulation, cell-wall composition and active transport.

ABSTRACT

Toxic concentrations of aluminium cations and low phosphorus availability are the main yield-limiting factors in acidic soils, which represent half of the potentially available arable land. *Brachiaria* grasses, which are commonly sown as a forage in the tropics because of their resilience and low demand for nutrients, have a greater tolerance to high concentrations of aluminium cations than most other grass crops. In this work, we explored the natural variation in tolerance to aluminium cations (Al^{3+}) between high and low tolerant *Brachiaria* species and characterised their transcriptional differences during stress. We also identified three QTLs associated with root vigour during Al^{3+} stress in their hybrid progeny. By integrating these results with a new *Brachiaria* reference genome, we have identified 30 genes responsible for Al^{3+} tolerance in *Brachiaria*. We also observed differential expression during stress of genes involved in RNA translation, response signalling, cell wall composition and vesicle location genes homologous to aluminium-induced proteins involved in limiting uptake or localizing the toxin. However, there was limited regulation of malate transporters in *Brachiaria*, which are associated with external tolerance mechanisms to Al^{3+} stress in other grasses. The contrasting regulation of RNA translation and response signalling suggests response phasing is critical to Al^{3+} tolerance.

KEYWORDS: Acid soils, Aluminium tolerance, *Brachiaria*, genome assembly, differential expression, QTL mapping, grass, *Urochloa*

INTRODUCTION

Acidic soils constitute approximately 30 % of the world's total land area and 50 % of the potentially available arable land (Von Uexküll and Mutert, 1995). Acidic soils are particularly predominant in a northern "temperate belt" and a southern "subtropical belt". Therefore, a broad range of vegetable, cereal and forage crops can be yield-limited in these conditions (Hede *et al.*, 2001). The adverse effects of soil acidity are mostly associated with several mineral toxicities and deficiencies, particularly increased concentrations of soluble forms of manganese, iron and aluminium, and reduced levels of available forms of phosphorus, calcium, magnesium and potassium. Among these, lower phosphorus solubility and aluminium toxicity are considered the main limiting factors on productivity (Eswaran *et al.*, 1997). As soil pH decreases below 5, aluminium becomes soluble as the aluminium trivalent cation (Al^{3+}), a form highly toxic to plants. Soluble Al^{3+} effect on root apices results in diminished ion and water uptake.

Although acid soils can be conditioned for improved agricultural use through the addition of lime, in general, the most sustainable strategy is a combination of agronomic practices and growing tolerant cultivars. Natural variation in aluminium tolerance has been identified for a number of crops with rice (*Oryza sativa*) being the most aluminium-tolerant among the food staples (Rao *et al.*, 2016). All *Brachiaria* (Trin.) Griseb. (syn. *Urochloa* P. Beauv.) species show greater tolerance to Al^{3+} toxicity than most other grass crops, including maize (*Zea mays*), rice or wheat (*Triticum aestivum*) (Kochian *et al.*, 2015).

Brachiaria grasses are native to East Africa and are widely sown as a forage to feed ruminants across the tropics, particularly in areas with marginal soils. *Brachiaria* has a set of desirable genetic characteristics linked to drought and waterlogging tolerance, poor and acidic soils tolerance, and resistance to major diseases. However, *Brachiaria* resilience is principally a result of low demand for soil nutrients (Pizarro *et al.*, 2013). As a consequence, toxic cation levels (and not reduced levels of mineral solutes) are the limiting factors on *Brachiaria* species productivity in acidic soil conditions.

88 Al^{3+} tolerance has been established to be a multigenic trait, though major genes can
89 also be important (Kochian *et al.*, 2015; Ryan *et al.*, 2009). The incomplete transfer of
90 tolerance from parents to near-isogenic lines in sorghum (*Sorghum bicolor*) (Melo *et*
91 *al.*, 2013), maize (Guimaraes *et al.*, 2014), and wheat (Johnson *et al.*, 1997; Tang *et*
92 *al.*, 2002) supports polygenic inheritance of Al^{3+} resistance.
93
94 Al^{3+} tolerance mechanisms are classified as external and internal tolerance
95 mechanisms (Furlan *et al.*, 2018; Kochian *et al.*, 2015). In the first group, plants
96 prevent Al^{3+} uptake by raising the pH in the rhizosphere or forming binding complexes
97 by exudation of citrate, malate and oxalate. In the second group, Al^{3+} is absorbed and
98 localized to cell organelles or the apoplast. In the tolerant rice variety Nipponbare, both
99 exclusion mechanisms and internal detoxification are important in withstanding
100 toxicity, while primarily internal detoxification occurs in the sensitive rice variety Modan
101 (Roselló *et al.*, 2015).
102
103 Little is known about the genetic basis of Al^{3+} tolerance in *Brachiaria*. Nevertheless,
104 screening experiments have evidenced different but consistent aluminium tolerance
105 among *Brachiaria* species and cultivars, which indicates the genetic basis of the trait
106 (Arroyave *et al.*, 2013). The three most important commercial species, *Brachiaria*
107 *brizantha* (A.Rich.) Stapf., *B. decumbens* Stapf., and *B. humidicola* (Rendle) Schweick
108 exist primarily as apomicts with varying levels of polyploidy (Valle and Savidan, 1996).
109 The diploid sexual species *B. ruziziensis* (Germ. & C.M. Evrard) is also used in
110 breeding as a bridge between apomictic species (Miles, 2007). *B. decumbens* is
111 significantly more tolerant to Al^{3+} than *B. ruziziensis* (Arroyave *et al.*, 2011; Bitencourt
112 *et al.*, 2011).
113
114 *Brachiaria* is one of the most widely used and promising forage genera in the American
115 and African tropics. For the potential of this species to be realised, it is important that
116 varieties are tailored to the particular demands of each environment in which it is
117 grown (Bailey-Serres *et al.*, 2019). While genomic approaches can accelerate genetic
118 gain from crop breeding, these approaches rely on resources that are costly and often
119 scarce in “orphan crops”. As part of this project, we have also consequently produced
120 some of the fundamental genomic resources previously absent for *Brachiaria*,
121 uniquely a reference genome. We have applied these new genomic resources to

122 develop a better understanding of the molecular basis of a key trait affecting *Brachiaria*
123 productivity, namely Al^{3+} tolerance.
124
125
126 **METHODS**
127
128 **Plant materials and phenotyping**
129
130 The interspecific mapping population used in this work consisted of 169 genotypes of
131 F1 progeny from a cross between the synthetic autopolyploid *B. ruziziensis* accession
132 BRX 44-02 and the segmental allopolyploid *B. decumbens* accession CIAT 606 (cv.
133 Basilisk). This population was generated initially to create saturate linkage maps and
134 identify markers linked to apomixis (Worthington *et al.*, 2016). Accessions were
135 phenotyped for aluminium tolerance at CIAT in Cali, Colombia, following Wenzl *et al*.
136 (2006). Briefly, the experiment consisted of six cycles (replications over time) with 1-7
137 replicate plants per cycle. Plants were grown for 20 days in hydroponic solutions with
138 0 or 200 μM $AlCl_3$ and phenotyped in each condition (control -C- and Al^{3+} stress -A-)
139 for cumulative root length (RLC and RLA), root biomass (RBC and RBA), and root tip
140 diameter (RDC and RDA) at the end of each experimental cycle. Data were
141 transformed to meet the assumption of normality; root length and biomass were
142 square-root transformed and root tip diameter was natural log-transformed. The
143 PROC MIXED method (SAS v. 9.2, Cary, NC) was used to fit a totally random effect
144 model. Genotypic best linear unbiased predictors (BLUPs) were calculated from stress
145 (200 μM $AlCl_3$) and control (0 μM $AlCl_3$) conditions individually and back transformed
146 to calculate relative root length (RRL), relative root biomass (RRB), and relative root
147 tip diameter (RRD) ratios.
148
149 **Genome sequencing, assembly and annotation**
150
151 We selected the *B. ruziziensis* genotype CIAT 26162 (2n = 2x = 18) as the source of
152 genomic DNA. This is a semi-erect diploid accession from Burundi (-3.1167, 30.1333)
153 that is believed to have been mutagenised with colchicine to produce the synthetic
154 autotetraploid *B. ruziziensis* BRX 44-02, one of the progenitors of the interspecific
155 mapping population analysed. The ploidy of CIAT 26162 has recently been verified by

156 cytogenetics (*P. Tomaszewska, personal comm.*). Two paired-end libraries were
157 created and sequenced in Illumina HiSeq 2500 machines in rapid run mode by the
158 Earlham Institute (approx. 70X) and the Yale Center for Genome Analysis (approx.
159 30X). Additionally, a Nextera mate-pair (MP) library with insert length of 7 Kb was
160 sequenced to improve the scaffolding. Read quality was assessed, and contaminants
161 and adaptors removed. Illumina Nextera MP reads were required to include a fragment
162 of the adaptor to be used in the following steps (Leggett *et al.*, 2013a). The pair-end
163 shotgun libraries were assembled and later scaffolded using the MP library with
164 Platanus v1.2.117, which is optimized for heterozygous genomes (Kajitani *et al.*,
165 2014). We did not use Platanus' gap-closing step. Approximately 1 million Pacbio
166 reads from this same genotype were generated in a PacBio RSII sequencer and used
167 for gap filling using PBJelly v.15.8.24 (English *et al.*, 2012). Scaffolds shorter than 1
168 Kbp were filtered out. We used 31mer spectra analysis to compare the assemblies
169 produced by different pipelines, as well as our final assembly with the assemblies from
170 preceding steps. A K-mer spectrum is a representation of how many fixed-length
171 words or K-mers (y-axis) appear a certain number of times or coverage (x-axis). The
172 K-mer counting was performed with KAT (Mapleson *et al.*, 2016). The completeness
173 of the assembly was checked with BUSCO (Simão *et al.*, 2015).
174
175 Repetitive and low complexity regions of the scaffolds were masked using
176 RepeatMasker (Tarailo-Graovac and Chen, 2009) based on self-alignments and
177 homology with the RepBase public database and specific databases built with
178 RepeatModeler (Smit and Hubley, 2008). Long terminal repeat (LTR)
179 retrotransposons were detected by LTRharvest (Ellinghaus *et al.*, 2008) and classified
180 with RepeatClassifier. The 5′ and 3′ ends of each LTR were aligned to each other with
181 MUSCLE (Edgar, 2004) and used to calculate the nucleotide divergence rate with the
182 Kimura-2 parameter using MEGA6 (Tamura *et al.*, 2013). The insertion time was
183 estimated by assuming an average substitution rate of 1.3×10^{-8} (Schmutz *et al.*, 2014)
184
185 Our annotation pipeline (De Vega *et al.*, 2015) uses four sources of evidence: (a) *De*
186 *novo* and genome-guided *ab initio* transcripts deduced from RNA-Seq reads from the
187 *B. ruziziensis* genotype assembled with Trinity (Grabherr *et al.*, 2011) and Tophat and
188 Cufflinks (Trapnell *et al.*, 2012), (b) gene models predicted by Augustus (Stanke *et al.*,
189 2006), (c) homology-based alignments of transcripts and proteins from four close

190 species with Exonerate and GMAP (Wu *et al.*, 2016), and (d) the repeats annotation.
191 Finally, MIKADO (Venturini *et al.*, 2018) built the gene models to be compatible with
192 this previous information. Proteins were compared with the NCBI non-redundant
193 proteins and EBI's InterPro databases and the results were imported into Blast2GO
194 (Conesa *et al.*, 2005) to annotate the GO and GO slim terms, enzymatic protein codes
195 and KEGG pathways. Proteins were also functionally annotated with the GO terms of
196 any significant orthologous protein in the eggNOG database (Powell *et al.*, 2014),
197 using the eggNOG-mapper pipeline (Huerta-Cepas *et al.*, 2017).
198
199 **Comparative genomics**
200
201 Syntenic blocks between *B. ruziziensis* and foxtail millet (*Setaria italica* (L.) P. Beauv)
202 whole genomes were identified with Minimap (Li, 2016), and plotted with D-GENIES
203 (Cabanettes and Klopp, 2018). Previously, we filtered out any scaffold shorter than 10
204 Kbp that did not contain any gene. The assembly was anchored to foxtail millet by
205 assigning each scaffold to the chromosome position where it had the longest
206 alignment chain after combining proximal alignments. For clustering, proteins from five
207 related species were assigned to eggNOG orthologous groups as before. A
208 phylogenetic tree based on these data was built with MUSCLE by aligning the
209 orthologous proteins within each eggnog cluster, filtering sets with one member per
210 specie (*P. virgatum* was excluded from this analysis), and finally estimating the
211 nucleotide divergence rate using MEGA v6, as before.
212
213 **Population genotyping and genetic map construction**
214
215 Genotyping-by-sequencing libraries were prepared and sequenced for the 169 F1
216 progenies and the two parents as described in Worthington *et al.* (2016). Reads were
217 demultiplexed according to the forward and reverse barcodes used during library
218 preparation with FastGBS (Torkamaneh *et al.*, 2017) and adaptors and enzymatic
219 motifs removed with Cutadapt (Martin, 2011). Reads were aligned to the genome
220 using BWA MEM (Li, 2013). SNP calling was done for each sample with GATK's
221 Haplotycaller (Van der Auwera *et al.*, 2013) without the duplicated read filter (-drf
222 DuplicateRead) and recalled for the population with GATK's GenotypeGVCFs, in both
223 tools with "--ploidy 4". In agreement with filtering criteria previously tested in tetraploid

224 *Brachiaria* samples (Worthington *et al.*, 2016), we used SNPs only, and required at
225 least 12 reads to call a homozygous site in any sample and a minimum allele
226 frequency of 5 %. We removed any site not called in a progenitor or in more than 20 %
227 of the progeny. Markers that were heterozygous in only one parent and had a
228 segregation ratio of a heterozygote to homozygote progeny of approximately 1:1
229 (between 0.5 and 1.75) were classified as single-dose allele (SDA) markers and used
230 in the linkage map construction. Separate genetic linkage maps of BRX 44-02 and
231 CIAT 606 were constructed in JoinMap v5 (Van Ooijen, 2011) using a threshold
232 linkage logarithm of odds (LOD) score of 10 to establish linkage groups. Marker order
233 was then determined using regression mapping with default settings. Downstream
234 QTL analysis with MapQTL 6 (Van Ooijen and Kyazma, 2009) was conducted using
235 only the *B. decumbens* CIAT 606 map.
236
237 **RNA-seq sequencing and analysis**
238
239 Two replicate plants of *B. decumbens* CIAT 606 (cv. Basilisk) and *B. ruziziensis* BRX
240 44-02 were grown in high aluminium (200 μM $AlCl_3$) and control (0 μM $AlCl_3$) conditions
241 in the greenhouse, as described previously. After three days of growth, roots and
242 leaves were harvested from each plant. RNA extraction was performed with RNeasy
243 Plant Mini kit (Qiagen, CA, USA) and sent to the sequencing service provider (Earlham
244 Institute, Norwich, UK) where Illumina RNA-seq libraries were prepared and
245 sequenced using the HiSeq 2500 platform. Sixteen libraries were independently
246 generated and sequenced: two tissues (roots and leaves), from two species (*B.*
247 *ruziziensis* and *B. decumbens*), in two conditions (0 and 200 μM $AlCl_3$ hydroponic
248 solutions), and two replicates. Contaminations in the raw data were discarded with
249 Kontaminant (Leggett *et al.*, 2013b). Adaptors were removed with Cutadapt (Martin,
250 2011) and quality checked with FastQC. Reads were mapped to the assembled
251 genome using STAR (Dobin *et al.*, 2013) and the gene models annotation for
252 guidance. Counts were estimated with Stringtie (Pertea *et al.*, 2015). We used DEseq
253 v2 (Love *et al.*, 2014) for analysing differential expression. Enriched GO terms and
254 other categories in each group of differentially expressed genes were identified in R
255 using TOPGO (Alexa and Rahnenfuhrer, 2010) using a Fisher's test (FDR<0.05) and
256 the "weight01" algorithm. The relation among GO terms was plotted in R using ggplot
257 (Wickham and Chang, 2008). We also reanalysed using this pipeline the publicly

258 available data (PRJNA314352) from Salgado *et al*. (2017), obtained from harvested
259 root tips from 12 day-old *B. decumbens* cv. Basilisk seedlings screened in similar
260 experimental conditions to those described in our study but after 8 hours of treatment
261 (instead of 72 hours).
262
263 **RESULTS**
264
265 **Root morphology in *Brachiaria* species in different aluminium cation**
266 **concentrations**
267
268 We demonstrated the superior aluminium tolerance of the *B. decumbens* accession
269 CIAT 606 compared with *B. ruziziensis* accession BRX 44-02 (Figure 1). The root
270 morphology of CIAT 606 was less affected than BRX 44-02 after growing for 20 days
271 in high aluminium (200 μM $AlCl_3$) and control (0 μM $AlCl_3$) concentration hydroponic
272 solutions. Under stress conditions, the roots of *B. decumbens* were over three times
273 as long and had twice the biomass of *B. ruziziensis.* However, the root tip diameter
274 increased in stress conditions in a similar ratio in both species (Supplementary table
275 S1).
276
277 The interspecific progeny obtained by crossing aluminium-tolerant *B. decumbens*
278 accession CIAT 606 and aluminium-sensitive *B. ruziziensis* accession BRX 44-02
279 showed segregation in cumulative root length (RL), root biomass (RB), and root tip
280 diameter (RD) (Figure 2; Supplementary File 1). We obtained highly significant
281 ($p < 0.001$) genotypic differences in control and stress conditions for the three traits
282 (RL, RB and RD). The root biomass ($r = 0.73$), length ($r = 0.76$) and diameter ($r = 0.69$)
283 of the progeny were significantly correlated when grown in stress (200 μM $AlCl_3$) and
284 non-stress (0 μM $AlCl_3$) conditions.
285
286
287 **Assembly and annotation of a *Brachiaria* reference genome**
288
289 A whole-genome assembly (WGA) of CIAT 26162 was produced using Platanus
290 v.1.2.4 (Kajitani *et al.*, 2014), from Illumina paired-end and Nextera mate-pair reads
291 with a coverage of approximately 100X and 7X, respectively (Supplementary table

292 S2). Platanus outperformed the contiguity results obtained with other pipelines.
293 Although the combination of ABySS for the contigs assembly and SOAP2 for the
294 scaffolding resulted in a larger assembly, a kmer frequency analysis (Mapleson *et al.*,
295 2016) evidenced that the additional content was repeated under-collapsed
296 heterozygosity that Platanus had purged instead (Supplementary figure S1). A gap-
297 filling step using approximately 1 million Pacbio reads with an average length of 4.8
298 Kbp resulted in a reduced percentage of ambiguous nucleotides (Ns) from 17.45 % to
299 11.39 %. We finally discarded all the sequences under 1 Kbp to produce the reference
300 genome we used for the downstream analysis (Table 1). To assess the completeness
301 of the assembly, we verified that 1,345 (93.4 %) of the 1,440 BUSCO orthologous
302 genes (Simão *et al.*, 2015) were present in the assembly; 1,216 of which were
303 completed and in a single copy, 32 were duplicated, and 97 were fragmented. This
304 WGA is deposited at NCBI with the accession number GCA_003016355. The raw
305 reads are deposited in the Bioproject PRJNA437375.
306
307 The repeat content (Supplementary table S3) was 51 % of the total genome
308 (656,355,643 bp, after excluding ambiguous bases, Ns), which is close to the 46 %
309 repeat content in foxtail millet (*Setaria italica* (L.) P. Beauv) (Zhang *et al.*, 2012). We
310 found a large number of *Gypsy* and *Copia* LTRs, which represent 24 % and 9.5 % of
311 the total genome excluding Ns. These transposons and proportions are also very
312 similar to those observed in foxtail millet. We compared the divergence between the
313 flanking tails in the LTRs (Supplementary figure S2) and identified a single very recent
314 burst of LTR *Gypsy* activity around 0.6 MYA (Kimura = 0.042 ± 0.026) and of LTR
315 *Copia* also around 0.6 MYA (Kimura = 0.041 ± 0.027). Other repeat elements,
316 including LINEs (Long Interspersed Nuclear Elements), simple repeat patterns of the
317 sequence, satellites, and transposons were much less common, except for En/Spm
318 DNA transposons observed in 4.2 % of the genome.
319
320 We annotated 42,232 coding genes, which included 42,359 predictive open reading
321 frames (ORFs), as well as 875 non-coding genes without a predicted ORF
322 (Supplementary file 2). Together these transcripts and non-coding genes define
323 43,234 targets for the expression analysis. 35,982 of the coding transcripts had a
324 homologous protein in the NCBI non-redundant (*nr*) database. In 58% of the cases,
325 the top hit was a *S. italica* sequence (Supplementary figure S3). Among those 35,982,

326 33,963 were functionally annotated with at least one GO term, and 39,488 had an
327 InterPro annotation. We also identified the best reciprocal hits with *Arabidopsis*
328 *thaliana*, rice, *Panicum halli* Vasey, foxtail millet, and *Setaria viridis* (L.) Beauv; and
329 the top homologous protein in Uniprot (Supplementary file 3). We aligned the
330 transcripts and proteins from five sequenced species in the subfamily Panicoideae,
331 foxtail millet, *S. viridis*, maize, *P. halli* and switchgrass (*P. virgatum* L.) on the WGA,
332 and found that on average 78 % and 72 % of the transcripts and proteins aligned with
333 an identity over 0.7, respectively (Supplementary table S4).
334
335
336 **Comparative genomics with related grasses**
337
338 We could assign 35,831 *Brachiaria* proteins to an eggNOG orthologous group (Powell
339 *et al.*, 2014), and 13,570 proteins could be further annotated with GO terms from the
340 eggNOG database. We also assigned the proteins from other species in the Poaceae
341 family to these eggNOG orthologous groups for Poaceae (poaVIR) in the eggNOG
342 database in order to identify shared clusters of proteins among these species
343 (Supplementary file 4; Supplementary figure S4). More than 70 % of the clusters of
344 proteins had double or triple the number of proteins in switchgrass than the other
345 species because of relatively recent whole-genome duplication events
346 (Supplementary table S5). Approximately 20 % of the clusters in maize and *B.*
347 *ruziziensis* had two proteins. From this analysis, we also estimated that there are
348 approximately two thousand proteins in other close species that were missed in our
349 *Brachiaria* assembly.
350
351 We estimated the divergence between these species based on the Kimura divergence
352 values between pairs of orthologous proteins in 6,450 clusters of proteins that included
353 only one member from each species (*P. virgatum* was excluded from this analysis;
354 Supplementary figure S5). By assuming an average substitution rate of two-times
355 (diploid) 1.3×10^{-8} (Schmutz *et al.*, 2014), we estimated that *Brachiaria* diverged from
356 the other Paniceae genera, *Setaria* and *Panicum*, around 13.4-15.5 million years ago
357 (MYA), while the split of the Paniceae and Andropogonodae tribes of subfamily
358 Panicoideae took place around 23.8-26.3 MYA (Supplementary figure S6).
359

360 The 23,076 scaffolds in the WGS longer than 10 Kbp or with at least one annotated
361 gene (533.9 Mbp) were aligned with the nine chromosomes of foxtail millet, the closest
362 relative with a high quality sequenced genome (Zhang *et al.*, 2012). Up to 21,145 of
363 the 23,076 scaffolds (91.6 %), which comprise 525.1 Mbp, could be aligned (Figure 3;
364 Supplementary file S5). Furthermore, we assigned chromosomal positions to 41,847
365 coding genes (41,974 transcripts) contained in these anchored sequences
366 (Supplementary file S6). We identified 59 synteny blocks, 36 of which were longer than
367 1 Mbp in both species (Figure 3). There were three large translocations when
368 comparing the foxtail millet and *B. ruziziensis* genomes between chromosomes 1 and
369 7, 2 and 6, as well as 3 and 5. Four inversions (smaller than the translocations) were
370 identified between tails in chromosomes 1 and 4 (both ends), 2 and 9 (proximal end),
371 and 2 and 3 (proximal end).
372
373 **QTL mapping in the interspecific *B. ruziziensis* X *B. decumbens* population**
374
375 Between 78.8 and 91.5 % of the Genotyping-by-sequencing (GBS) reads from each
376 169 interspecific progeny and the parents could be aligned in the assembly. After
377 filtering, there were an average of 81,831 SNPs and 15,595 indel sites per sample. In
378 total, 799,155 polymorphic sites were called in the population, 85.7 % of these sites
379 were SNPs. After filtering, 15,074 SNP sites were homozygous in the female parent
380 (*B. ruziziensis* BRX 44-02) and heterozygous in the male parent (*B. decumbens* CIAT
381 606) (annotated as nnxnp markers in Joinmap), 4,891 sites were heterozygous in only
382 the female parent (lmxll), and 1,652 were heterozygous in both parents (hkxhk). We
383 classified 4,817 nnxnp and 1,252 lmxll sites as single dose alleles (SDAs, or "simplex"
384 markers) based on their 1:1 heterozygous/homozygous segregation ratio in the
385 progeny and used them in the genetic map construction. We used in our analysis the
386 genetic map of the male parent (*B. decumbens* CIAT 606), which included 4,427
387 markers placed in 18 linkage groups (Supplementary figure S7, Supplementary file 7).
388 This corresponds with the number of base chromosomes expected in an allotetraploid
389 (2n = 4x = 36) *Brachiaria* population. Linkage groups had an average length of 74.7 ±
390 22.7 cM. Using the same raw data, a join genetic map of both parents and composed
391 of 36 linkage groups was generated in Worthington *et al*. (2016). Two linkage groups
392 were assigned to each the nine base chromosomes of *B. ruziziensis* based on
393 alignments of each SNP to the WGA and named following the numbering system used

394 for foxtail millet. We also aligned the WGA scaffolds with the genetic map to compare
395 the co-linearity between the position of each marker in the genetic map and genome
396 assembly (Supplementary file S7).
397
398 QTL mapping was performed to identify genetic regions associated with root length
399 (RL), biomass (RB) and root tip diameter (RD) under control and Al^{3+} stress conditions
400 in the interspecific mapping population. Three hundred and seventy-one markers had
401 an LOD over 3 associated with one or more of the traits. Two hundred and twelve
402 WGS scaffolds contained at least one marker with LOD over 3 (Supplementary file 7).
403
404 Three significant QTL were identified (Figure 4). The first QTL, which peaked at 5.22,
405 12.65, 25.797 and 26.027 cM and extended from 5.22 to 32.481 cM on LG 1 (Chr 8),
406 was associated with root length and biomass under control and Al^{3+} stress conditions
407 but not with relative root length or relative root biomass. The second QTL, which
408 peaked at 79.738 and 96.802 cM and extended from 79.738 to 98.851 cM on LG 3
409 (Chr 7) was associated with relative root length, root tip diameter under Al^{3+} stress
410 conditions, and relative root tip diameter. The last QTL extended from 49.12 to 62.127
411 cM (peak at 50.423 cM) on LG 4 (Chr 3) and was only associated with relative root tip
412 diameter. These three QTLs each explained from 12.8 % to 16.1% of the phenotypic
413 variance for the associated traits (Supplementary table S6).
414
415
416 **Transcriptional differences during stress between *Brachiaria* species**
417
418 We performed RNA-seq from stem and root tissue samples extracted from *B.*
419 *decumbens* CIAT 606 and *B. ruziziensis* BRX 44-02 after growing for three days in
420 control (0 μM $AlCl_3$) or high (200 μM $AlCl^3$) aluminium cation concentration hydroponic
421 solutions. When the normalised counts for all the genes were used to cluster the
422 samples, these clusters firstly grouped by tissue, secondly by genotype, and thirdly by
423 treatment (Supplementary figure S8). There were 4,481 differentially expressed (DE)
424 genes in total, with 3,996 of these differentially regulated in a single genotype and
425 tissue (Figure 5). Among these 4,481 DE genes, 4,162 genes were DE in roots only,
426 265 in stems only, and 54 in both tissues.
427

428 The three QTL regions contained 918 genes; 581 in LG1, 153 in LG3, and 184 in LG4.
429 Of these 918, 84 were DE genes (Supplementary file 8). Twenty-seven DE genes
430 were annotated as membrane components, 21 were annotated as involved in
431 response to hormones or biotic/abiotic stress, and 23 were annotated as binding to
432 different molecular compounds, including ATP/ADP/GTP, metal ions and DNA. 34 of
433 the 87 genes were not annotated with one of these previous GO terms, but several
434 were annotated with several GO terms.
435
436 An enrichment analysis of GO terms over-represented among DE genes in each
437 species allowed us to identify the biological processes (BP) and molecular functions
438 (MF) that are similarly or differently regulated among them. After annotating the genes
439 with the full set of GO terms (Supplementary figure S9 and S10), we also simplified
440 the results to "GO slim" terms, contain the subset of higher-level terms from the GO
441 resource (Figure 6; Supplementary Table S7). For the enrichment analysis we
442 considered the either up-regulated or down-regulated genes in each sample. There
443 was limited overlap among GO terms based on the DE genes included in each term
444 (Supplementary figure S11).
445
446 Five MF terms related to RNA/mRNA/rRNA binding with the ribosome (MF:3723,
447 3729, 19843; and 3735 and 5198) and two BP terms, "translation" and
448 "ribonucleoprotein complex assembly" (BP: 6412, 22618), were significantly enriched
449 among down-regulated during stress genes in *B. ruziziensis* (146 genes) and *B.*
450 *decumbens* (39 genes).
451
452 Genes annotated as "transmembrane transporters" (MF:22857) were highly over-
453 represented among up-regulated during stress DE genes (44 in *B. decumbens* and 70
454 in *B. ruziziensis*). Fifteen DE transmembrane transporters were common to both
455 species, and five were annotated as induced by aluminium and are later discussed.
456
457 Several GO terms showed contrasting regulation between both species. E.g. "Cell wall
458 organization and biogenesis" was enriched in both species and included 51 down-
459 regulated DE genes in *B. ruziziensis*, but 17 up-regulated DE genes in *B. decumbens*.
460 Most of these genes were peroxidases and expansin proteins induced by various plant
461 hormones (e.g. ethylene, GA, auxin) and involved in toxin removal during oxidative

462 stress (Kochian *et al.*, 2015). The GO term “glycosyl hydrolase” was also enriched
463 among down-regulated genes in *B. ruziziensis* (39 genes), but among up-regulated
464 genes in *B. decumbens* (18 genes). Most of the genes annotated as “Glycosyl
465 hydrolases” were also annotated as involved in the “carbohydrate metabolism”
466 (BP:5975).
467
468 Several of the DE genes that exhibited high fold-changes in both species were
469 involved in phospholipid, phosphate, magnesium, auxin, nitrate and miRNA transport
470 in the cell (Genes 6944G2, 12087G2, 8068G4, 26018G2, 4534G2, 2708G4).
471
472 By reanalysing the data from Salgado *et al*. 2017, we could also compare the enriched
473 GO terms between *B. decumbens* cv. Basilisk exposed to 200 µM $AlCl_3$ for 8 hours
474 and 72 hours (Supplementary Figure S12 and Supplementary Table S7). This
475 comparison evidenced differences between 8 hours and 72 hours in the same
476 genotype in GO terms related to RNA translation and response to stress (BP:6950),
477 among others.
478
479
480 **DISCUSSION**
481
482 **Forward genetics and newly produced genomic resources to identify candidate**
483 **loci for abiotic stress tolerance**
484
485 The negative effects of soil acidity on crop production are associated with different
486 mineral toxicities and deficiencies. Aluminium cation toxicity has long been established
487 to be the single most important limiting factor of acidic soil productivity (Eswaran *et al.*,
488 1997). All *Brachiaria* species show some tolerance to Al^{3+} toxicity, particularly
489 compared with other grasses such as wheat, rice and maize (Arroyave *et al.*, 2013;
490 Kochian *et al.*, 2015). While most crops reduce root growth to 50 % when exposed to
491 5 µM Al^{3+}, *Brachiaria* species need to be exposed to up to 35 µM to exhibit a reduced
492 root growth of 25 % (Poschenrieder *et al.*, 2008).
493
494 Natural adaptation to acid soils can be measured by estimating root vigour in low pH
495 conditions and tolerance to high concentrations of Al^{3+} (Wenzl *et al.*, 2006). In our

496 experiment, *B. decumbens* CIAT 606 (cv. Basilisk) root morphology was less affected
497 than *B. ruziziensis* BRX 44-02 after growing for 20 days in control and high 200 μM
498 Al^{3+} concentration hydroponic solutions. As a comparison, in a 21-day long term study
499 using a similar experimental protocol, four *B. decumbens* and four *B. ruziziensis*
500 genotypes showed intermediate tolerance of Al^{3+}, one *B. ruzizensis* genotype was
501 sensitive, and only the *B. decumbens* cultivar Basilisk was unaffected by high Al^{3+}
502 (Bitencourt *et al.*, 2011). Interestingly, Furlan *et al.* (2018) recently reported a higher
503 Al^{3+} tolerance in *B. brizantha* cv. Xaraes than in *B. decumbens* cv. Basilisk.
504
505 The three QTLs we identified were of moderate effect (LOD scores under 6, each
506 accounting 12.8 % to 16.1% of observed phenotypic variance), but were observed for
507 several root traits. DE genes in the QTLs highlighted a link with membrane transport
508 (including metal ions), regulation and signalling (binding to DNA), and energy
509 (carbohydrate metabolism and binding to ATP/ADP/GTP) molecular mechanisms in
510 the three QTLs. The three QTLs were associated with similar molecular functions.
511 Eight genes in the QTL were DE in both species, including two metal-binding
512 transmembrane P450 cytochromes (8440G2 and 598G8), one root-exclusive
513 potassium ion membrane transporter (94G8) induced by potassium starvation
514 (Banuelos *et al.*, 2002), a cysteine XCP1 protease (869G16) that may have a
515 developmental senescence specific cell death function during apoptosis and heavy
516 metal detoxification (De Michele *et al.*, 2009), and a protein (8234G4) not found in
517 other related species.
518
519 We are also making publicly available the genome assembly and gene annotation of
520 a diploid accession of *B. ruziziensis*. This diploid accession collected in Burundi is
521 likely the genotype that was mutagenised with colchicine to produce CIAT BRX 44-02,
522 the autotetraploid *B. ruziziensis* progenitor of the interspecific population analysed in
523 this study. Our transcriptomic study and comparative genomics analysis are examples
524 of its utility. While tetraploid *Brachiaria* are the main accessions used for breeding, we
525 opted for a non-polyploid diploid accession because *Brachiaria* grasses are
526 heterozygous outcrossing species.
527
528 The assembly was partially scaffolded to the pseudomolecule level using a genetic
529 linkage map of *B. decumbens* CIAT 606 containing approximately 5,000 markers. This

530 genetic map had previously been assembled without a genome (Worthington *et al.*,
531 2016), but a higher number of markers were incorporated by conducting SNP calling
532 using this new reference. The incorporation of long reads could improve this assembly
533 and allow for polyploid *Brachiaria* genome references in the near future. Because of
534 the limited number of markers, almost all the scaffolds were also placed on the high-
535 quality foxtail millet genome. While we identified three large chromosomal
536 translocations, there was a very high collinearity between the two species as
537 previously observed (Worthington *et al.*, 2016) and as might be predicted from species
538 that we quantified diverged "only" 13-15 MYA.
539
540
541 **Differentially expressed genes associated with internal tolerance mechanisms**
542 **to Al^{3+} in *Brachiaria***
543
544 Aluminium internal tolerance mechanisms involve either modification of the properties
545 of the root cell wall, or the uptake and sequestration of Al^{3+} once it enters the plant
546 (Kochian *et al.*, 2015). Ramos *et al.* (2012) observed that *B. decumbens* accumulated
547 Al^{3+} in the mucilage layer of root apices, which reduced the quantity of Al^{3+} reaching
548 the cell wall and crossing the plasma membrane. Arroyave *et al.* (2013) suggested
549 that the presence of a complex exodermis in *B. decumbens*, absent in *B. ruziziensis*,
550 may contribute to a more efficient exclusion of Al^{3+}. On the other hand, a higher
551 concentration of root pectin measured in *B. ruziziensis* during stress could evidence
552 increased apoplastic aluminium binding (Horst *et al.*, 2010).
553
554 Changes in the structural properties of cell wall carbohydrates are mediated by
555 expansins, endo-β-1,4-glucanases, xyloglucan transferases and hydrolases (XTH)
556 (e.g. AtXTH31 and AtXTH15) and pectin methylesterases (Kochian *et al.*, 2015; Yang
557 *et al.*, 2011). Contrasting regulation (Up-regulated in one species but down-regulated
558 in the other) in enriched GO terms between *B. decumbens* and *B. ruziziensis,*
559 suggests different regulation of genes associated with xyloglucan transfer
560 (GO:16762), glycosyl hydrolase (MF:16798) and oxidation (GO:52716). This
561 contrasting enrichment was largely due to 12 XTH proteins that were down-regulated
562 during stress in *B. ruziziensis*, but not in *B. decumbens*. One of them (5400G2) was
563 located in the QTL region on LG1 (Chr 8). There were three additional differentially

564 expressed XTH proteins that were up-regulated during stress: 5233G2 (AtXTH23) only
565 in *B. decumbens*, and 6544G2 (AtXTH32) and 11683G4 (AtXTH27) in both *B.*
566 *decumbens* and *B. ruziziensis*. Related to this, AtSLK2 is involved in cell wall pectin
567 methylesterification in response to Al^{3+} stress (Geng *et al.*, 2017). The *Brachiaria*
568 homologous gene to SLK2 (1984G2) was up-regulated in both *B. ruziziensis* and *B.*
569 *decumbens*, but only DE under stress in *B. decumbens*.
570
571 Once Al^{3+} has entered the root, the uptake and sequestration of Al^{3+} includes
572 molecular binding and eventually compartmentation of the toxin. ALS (Aluminium
573 Sensitive) transporters and NRAM metal ion transporters have been proposed as the
574 key proteins in Al^{3+} localization to the tonoplast and other cell organelles, and away
575 from the sensitive root tips in *A. thaliana* and rice (Huang *et al.*, 2010; Huang *et al.*,
576 2012; Larsen *et al.*, 2007). Specifically, an NRAM aluminium transporter (NRAT1)
577 localized in the plasma membrane appears to be expressly involved in storing Al^{3+} in
578 root vacuoles in rice and maize. In *Brachiaria*, we identified 21 NRAM proteins, but
579 only three of them were DE: the homologous gene (2499G8) to OsTITANIA
580 (AtOBE3/ATT1), which is the transcription factor that functions as a regulator of NRAM
581 and other metal transporter genes (Tanaka *et al.*, 2018) and two of the three *Brachiaria*
582 proteins showing close homology to NRAT1 (3672G6 and 30107G2). These were
583 significantly up-regulated in both *B. decumbens* and *B. ruziziensis* during stress. Eight
584 genes in the *Brachiaria* genome are homologous to ALS1 and annotated as
585 aluminium-induced ABC transporters, but only one gene (3096G6) was up-regulated
586 during stress in *B. ruziziensis.*
587
588 In rice, the complex formed by STAR1 and STAR2/AtALS3 (Sensitive To Aluminium
589 Rhizotoxicity) is involved in aluminium-induced alterations of the cell wall composition
590 related to less aluminium-binding in the apoplast (Huang *et al.*, 2010; Huang *et al.*,
591 2009). These ABC transporters appear to mediate the efflux of UDP-glucose into the
592 cell wall, which could alter the cell wall composition and lead to a reduction in Al-
593 binding capacity (Kochian *et al.*, 2015). Fifteen proteins were homologous to
594 STAR/ALS in *Brachiaria*, but only two were DE: gene 8448G4 homologous to
595 OsSTAR1, and gene 7361G2 homologous to OsSTAR2. STAR1 and STAR2 were up-
596 regulated in both *B. ruziziensis* and *B. decumbens* during stress.
597

598

599 **Differentially expressed genes associated with external tolerance mechanisms**
600 **to Al^{3+} in *Brachiaria***

601

602 Most aluminium tolerant crops additionally rely on external restriction to prevent the
603 uptake of aluminium and its entry into the root cells through the release of anionic
604 organic acids in the rhizosphere that chelate the Al^{3+} (Kochian *et al.*, 2015; Rao *et al.*,
605 2016). However, *Brachiaria* appears to not rely on secreted organic acids since there
606 was no difference in secreted organic acids between *Brachiaria* species (Arroyave *et*
607 *al.*, 2013; Wenzl *et al.*, 2001). The lack of correlation between exudation and
608 resistance has also been observed in rice (Famoso *et al.*, 2010; Ma *et al.*, 2002).
609 Furthermore, tolerant *B. decumbens* accessions secreted 3-30 times less organic
610 acids than sensitive species such as maize and wheat (Arroyave *et al.*, 2018; Wenzl
611 *et al.*, 2001). However, while *B. decumbens* citrate exudation was about 200 times
612 lower than that observed in aluminium-tolerant rice, the same study evidenced high
613 oxalate exudation in *B. decumbens* roots, but only between 24 and 36 hours after
614 exposure to the toxic concentration (Arroyave *et al.*, 2018). It appears that other
615 mechanisms of resistance overshadow the impact of root exudation.

616

617 Two families of membrane transporters, aluminium-activated malate transporter
618 (ALMT) and the multidrug and toxic compound extrusion (MATE) family, are
619 responsible for plasma membrane malate and citrate efflux, respectively (Guimaraes
620 *et al.*, 2014; Raman *et al.*, 2005; Rao *et al.*, 2016). Citrate is a much stronger chelating
621 agent for Al^{3+} than malate (Ma, 2000). In *Brachiaria*, we identified three citrate MATE
622 proteins, which were homologous to FRDL (Ferric Reductase Defective Like) proteins
623 and up-regulated with large fold-changes in *B. decumbens* only (61G2), or in both
624 species (259G14 and 675G12). In rice, FRDL4 is responsible for aluminium-induced
625 citrate efflux required for external detoxification (Yokosho *et al.*, 2011).

626

627 We identified thirteen aluminium-activated malate transporters (AMLTs) in the
628 genome. However, only two were differentially expressed: 11634G4 was up-regulated
629 4.74 fold-change during stress in *B. decumbens*, and 462G24 was down-regulated
630 2.35 fold-change in *B. ruziziensis*. We identified a cluster with three contiguous non-
631 DE AMLTs (5136G2, 5136G4 and 5136G6) in scaffold 5136 (LG3 (Chr. 7): 71.83-

632 72.95 cM) around 10 cM from the QTL. This is consistent with the observation that
633 copy-number variation of ALMT correlated with aluminium resistance in rye and maize
634 (Collins *et al.*, 2008; Maron *et al.*, 2013).
635
636 C_2H_2-type zinc-finger transcription factors STOP1 (ART1 in rice) and STOP2 regulate
637 aluminium-induced expression of several MATE and ALMT genes in Arabidopsis and
638 rice (Iuchi *et al.*, 2007; Kobayashi *et al.*, 2014; Yamaji *et al.*, 2009). We identified three
639 transcription factors homologous to AtSTOP1, one DE in *B. ruziziensis* (29G2) and
640 another two (3833G12 and 243G34) which were not. We also identified two
641 transcription factors homologous to AtSTOP2, both DE with high fold-change in *B.*
642 *ruziziensis* and *B. decumbens* (126G26 and 1615G2). All five were homologous to
643 OsART1, the STOP1 homolog in rice, which up-regulated at least 31 genes in an Al-
644 dependent manner, including STAR1, FRDL, NRAMP proteins (Kochian *et al.*, 2015;
645 Yamaji *et al.*, 2009).
646
647 The "transmembrane transporters" GO term (MF:22857) were highly overrepresented
648 among up-regulated DE genes during stress in both species (44 genes in *B.*
649 *decumbens* and 70 genes in *B. ruziziensis*). Fifteen transmembrane transporters were
650 DE in both species, and five were annotated as induced by aluminium: NRAT1
651 (3672G6), STAR1 (8448G4), ALS3 (7361G2) and two citrate MATE transporter
652 (675G12 and 259G14). All these have been highlighted in our discussion, up-
653 regulated with high fold-changes in both species, and likely indispensable genes for
654 aluminium-tolerance in *Brachiaria*.
655
656 In this work we have presented a comprehensive analysis of the molecular mechanism
657 linked to aluminium tolerance in *Brachiaria* species. By assembling and annotating a
658 diploid genotype of *B. ruziziensis* we have developed the capability for genomic-based
659 studies of desirable phenotypic traits. Using this resource, we have identified three
660 QTLs associated to root architecture and vigour during Al^{3+} stress in a hybrid
661 population from a high and low tolerant accession. We have also identified a number
662 of genes and molecular responses that impact on different aspects of signalling, cell-
663 wall composition and active transports as response to aluminium stress. *Brachiaria*
664 tolerance appears to build in the same genes than in rice. However, we found that
665 external mechanisms such sequestration of Al^{3+} common in other grasses might be

666 not that important in *Brachiaria.* Also, contrasting regulation in the same genotype after
667 8 or 72 hours of Al^{3+} stress of numerous genes involved in RNA translation can explain
668 the different levels of tolerance among different Brachiaria species. The newly
669 annotated draft genome represents an important base upon which study other aspects
670 of *Brachiaria* biology.
671

672 **ACKNOWLEDGEMENTS**

673 This work was partially funded by a BBSRC's Global Challenge Research Fund
674 BB/P028098/1 and a BBSRC's Newton Fund Postdoctoral Twinning Award
675 BBS/OS/NW/000011.
676

677 **DATA AVAILABILITY**

678 Raw reads are deposited in SRA under accession PRJNA437375. The genome
679 assembly is deposit at NCBI with accession GCA_003016355.1; The genome
680 assembly, chromosomal anchoring in AGP format, and gene annotation in GFF3
681 format can also be downloaded as individual files
682 (http://dx.doi.org/10.5281/zenodo.3703092). Individual scaffolds can be accessed at
683 NCBI's GenBank accession numbers PVZT01000001 to PVZT01102577.
684
685

686 **REFERENCES**

687

688 **Alexa A, Rahnenfuhrer J**. 2019. topGO: enrichment analysis for gene ontology. R
689 package version **2.37.0**.
690 **Arroyave C, Barceló J, Poschenrieder C, Tolrà R**. 2011. Aluminium-induced
691 changes in root epidermal cell patterning, a distinctive feature of hyperresistance to
692 Al in *Brachiaria decumbens*. Journal of Inorganic Biochemistry **105**, 1477-1483.
693 **Arroyave C, Tolrà R, Chaves L, de Souza MC, Barceló J, Poschenrieder C**.
694 2018. A proteomic approach to the mechanisms underlying activation of aluminium
695 resistance in roots of Urochloa decumbens. Journal of Inorganic Biochemistry **181**,
696 145-151.
697 **Arroyave C, Tolrà R, Thuy T, Barceló J, Poschenrieder C**. 2013. Differential
698 aluminum resistance in *Brachiaria* species. Environmental and Experimental Botany
699 **89**, 11-18.
700 **Bailey-Serres J, Parker JE, Ainsworth EA, Oldroyd GE, Schroeder JI**. 2019.
701 Genetic strategies for improving crop yields. Nature **575**, 109-118.
702 **Banuelos MA, Garciadeblas B, Cubero B, Rodrıguez-Navarro A**. 2002. Inventory
703 and functional characterization of the HAK potassium transporters of rice. Plant
704 Physiology **130**, 784-795.
705 **Bitencourt GdA, Chiari L, Laura VA, Valle CBd, Jank L, Moro JR**. 2011.
706 Aluminum tolerance on genotypes of signal grass. Revista Brasileira de Zootecnia
707 **40**, 245-250.
708 **Cabanettes F, Klopp C**. 2018. D-GENIES: dot plot large genomes in an interactive,
709 efficient and simple way. PeerJ **6**, e4958.
710 **Collins N, Shirley N, Saeed M, Pallotta M, Gustafson J**. 2008. An ALMT1 gene
711 cluster controlling aluminum tolerance at the Alt4 locus of rye (*Secale cereale* L.).
712 Genetics **179**, 669-682.
713 **Conesa A, Götz S, García-Gómez JM, Terol J, Talón M, Robles M**. 2005.
714 Blast2GO: a universal tool for annotation, visualization and analysis in functional
715 genomics research. Bioinformatics **21**, 3674-3676.
716 **De Michele R, Vurro E, Rigo C, Costa A, Elviri L, Di Valentin M, Careri M, Zottini**
717 **M, di Toppi LS, Schiavo FL**. 2009. Nitric oxide is involved in cadmium-induced
718 programmed cell death in *Arabidopsis* suspension cultures. Plant Physiology **150**,
719 217-228.

720 **De Vega JJ, Ayling S, Hegarty M, Kudrna D, Goicoechea JL, Ergon Å, Rognli**
721 **OA, Jones C, Swain M, Geurts R**. 2015. Red clover (*Trifolium pratense* L.) draft
722 genome provides a platform for trait improvement. Scientific reports **5**, 17394.
723 **Dobin A, Davis CA, Schlesinger F, Drenkow J, Zaleski C, Jha S, Batut P,**
724 **Chaisson M, Gingeras TR**. 2013. STAR: ultrafast universal RNA-seq aligner.
725 Bioinformatics **29**, 15-21.
726 **Edgar RC**. 2004. MUSCLE: multiple sequence alignment with high accuracy and
727 high throughput. Nucleic acids research **32**, 1792-1797.
728 **Ellinghaus D, Kurtz S, Willhoeft U**. 2008. LTRharvest, an efficient and flexible
729 software for de novo detection of LTR retrotransposons. BMC Bioinformatics **9**, 18.
730 **English AC, Richards S, Han Y, Wang M, Vee V, Qu J, Qin X, Muzny DM, Reid**
731 **JG, Worley KC**. 2012. Mind the gap: upgrading genomes with Pacific Biosciences
732 RS long-read sequencing technology. PloS One **7**, e47768.
733 **Eswaran H, Reich P, Beinroth F**. 1997. Global distribution of soils with acidity. In:
734 Monis AC *et al.*, eds. Plant-Soil interactions at low pH, 159-164.
735 **Famoso AN, Clark RT, Shaff JE, Craft E, McCouch SR, Kochian LV**. 2010.
736 Development of a novel aluminum tolerance phenotyping platform used for
737 comparisons of cereal aluminum tolerance and investigations into rice aluminum
738 tolerance mechanisms. Plant Physiology **153**, 1678-1691.
739 **Furlan F, Borgo L, Rabêlo FHS, Rossi ML, Martinelli AP, Azevedo RA, Lavres J**.
740 2018. Aluminum-induced stress differently modifies *Urochloa* genotypes responses
741 on growth and regrowth: root-to-shoot Al-translocation and oxidative stress.
742 Theoretical and Experimental Plant Physiology **30**, 141-152.
743 **Geng X, Horst WJ, Golz JF, Lee JE, Ding Z, Yang ZB**. 2017. *LEUNIG_HOMOLOG*
744 transcriptional co-repressor mediates aluminium sensitivity through *PECTIN*
745 *METHYLESTERASE 46*-modulated root cell wall pectin methylesterification in
746 *Arabidopsis*. The Plant Journal **90**, 491-504.
747 **Grabherr MG, Haas BJ, Yassour M, Levin JZ, Thompson DA, Amit I, Adiconis**
748 **X, Fan L, Raychowdhury R, Zeng Q**. 2011. Full-length transcriptome assembly
749 from RNA-Seq data without a reference genome. Nature Biotechnology **29**, 644.
750 **Guimaraes CT, Simoes CC, Pastina MM, Maron LG, Magalhaes JV,**
751 **Vasconcellos RC, Guimaraes LJ, Lana UG, Tinoco CF, Noda RW**. 2014. Genetic
752 dissection of Al tolerance QTLs in the maize genome by high density SNP scan.
753 BMC Genomics **15**, 153.

754 **Hede A, Skovmand B, Lopez Cesati J**. 2001. Acid soils and aluminum toxicity.
755 Application of Physiology in Wheat Breeding. CIS-3160, CIMMYT.
756 **Horst WJ, Wang Y, Eticha D**. 2010. The role of the root apoplast in aluminium-
757 induced inhibition of root elongation and in aluminium resistance of plants: a review.
758 Annals of Botany **106**, 185-197.
759 **Huang C-F, Yamaji N, Ma JF**. 2010. Knockout of a bacterial-type ATP-binding
760 cassette transporter gene, AtSTAR1, results in increased aluminum sensitivity in
761 *Arabidopsis*. Plant Physiology **153**, 1669-1677.
762 **Huang CF, Yamaji N, Chen Z, Ma JF**. 2012. A tonoplast-localized half-size ABC
763 transporter is required for internal detoxification of aluminum in rice. The Plant
764 Journal **69**, 857-867.
765 **Huang CF, Yamaji N, Mitani N, Yano M, Nagamura Y, Ma JF**. 2009. A bacterial-
766 type ABC transporter is involved in aluminum tolerance in rice. The Plant Cell **21**,
767 655-667.
768 **Huerta-Cepas J, Forslund K, Coelho LP, Szklarczyk D, Jensen LJ, von Mering**
769 **C, Bork P**. 2017. Fast genome-wide functional annotation through orthology
770 assignment by eggNOG-mapper. Molecular Biology and Evolution **34**, 2115-2122.
771 **Iuchi S, Koyama H, Iuchi A, Kobayashi Y, Kitabayashi S, Kobayashi Y, Ikka T,**
772 **Hirayama T, Shinozaki K, Kobayashi M**. 2007. Zinc finger protein STOP1 is critical
773 for proton tolerance in *Arabidopsis* and coregulates a key gene in aluminum
774 tolerance. Proceedings of the National Academy of Sciences **104**, 9900-9905.
775 **Johnson JP, Carver BF, Baligar V**. 1997. Expression of aluminum tolerance
776 transferred from Atlas 66 to hard winter wheat. Crop Science **37**, 103-108.
777 **Kajitani R, Toshimoto K, Noguchi H, Toyoda A, Ogura Y, Okuno M, Yabana M,**
778 **Harada M, Nagayasu E, Maruyama H**. 2014. Efficient *de novo* assembly of highly
779 heterozygous genomes from whole-genome shotgun short reads. Genome research
780 **24**, 1384-1395.
781 **Kobayashi Y, Ohyama Y, Kobayashi Y, Ito H, Iuchi S, Fujita M, Zhao C-R,**
782 **Tanveer T, Ganesan M, Kobayashi M**. 2014. STOP2 activates transcription of
783 several genes for Al-and low pH-tolerance that are regulated by STOP1 in
784 *Arabidopsis*. Molecular Plant **7**, 311-322.
785 **Kochian LV, Piñeros MA, Liu J, Magalhaes JV**. 2015. Plant adaptation to acid
786 soils: the molecular basis for crop aluminum resistance. Annual Review of Plant
787 Biology **66**, 571-598.

788 **Larsen PB, Cancel J, Rounds M, Ochoa V**. 2007. *Arabidopsis* ALS1 encodes a
789 root tip and stele localized half type ABC transporter required for root growth in an
790 aluminum toxic environment. Planta **225**, 1447.
791 **Leggett RM, Clavijo BJ, Clissold L, Clark MD, Caccamo M**. 2013a. NextClip: an
792 analysis and read preparation tool for Nextera Long Mate Pair libraries.
793 Bioinformatics **30**, 566-568.
794 **Leggett RM, Ramirez-Gonzalez RH, Clavijo B, Waite D, Davey RP**. 2013b.
795 Sequencing quality assessment tools to enable data-driven informatics for high
796 throughput genomics. Frontiers in Genetics **4**, 288.
797 **Li H**. 2013. Aligning sequence reads, clone sequences and assembly contigs with
798 BWA-MEM. arXiv preprint:1303.3997.
799 **Li H**. 2016. Minimap and miniasm: fast mapping and de novo assembly for noisy
800 long sequences. Bioinformatics **32**, 2103-2110.
801 **Love MI, Huber W, Anders S**. 2014. Moderated estimation of fold change and
802 dispersion for RNA-seq data with DESeq2. Genome biology **15**, 550.
803 **Ma JF**. 2000. Role of organic acids in detoxification of aluminum in higher plants.
804 Plant and Cell Physiology **41**, 383-390.
805 **Ma JF, Shen R, Zhao Z, Wissuwa M, Takeuchi Y, Ebitani T, Yano M**. 2002.
806 Response of rice to Al stress and identification of quantitative trait loci for Al
807 tolerance. Plant and Cell Physiology **43**, 652-659.
808 **Mapleson D, Garcia Accinelli G, Kettleborough G, Wright J, Clavijo BJ**. 2016.
809 KAT: a K-mer analysis toolkit to quality control NGS datasets and genome
810 assemblies. Bioinformatics **33**, 574-576.
811 **Maron LG, Guimarães CT, Kirst M, Albert PS, Birchler JA, Bradbury PJ,**
812 **Buckler ES, Coluccio AE, Danilova TV, Kudrna D**. 2013. Aluminum tolerance in
813 maize is associated with higher MATE1 gene copy number. Proceedings of the
814 National Academy of Sciences **110**, 5241-5246.
815 **Martin M**. 2011. Cutadapt removes adapter sequences from high-throughput
816 sequencing reads. EMBnet Journal **17**, 10-12.
817 **Melo JO, Lana UG, Piñeros MA, Alves VM, Guimarães CT, Liu J, Zheng Y,**
818 **Zhong S, Fei Z, Maron LG**. 2013. Incomplete transfer of accessory loci influencing
819 SbMATE expression underlies genetic background effects for aluminum tolerance in
820 sorghum. The Plant Journal **73**, 276-288.

821 **Miles JW**. 2007. Apomixis for cultivar development in tropical forage grasses. Crop
822 Science **47**, S-238-S-249.
823 **Pertea M, Pertea GM, Antonescu CM, Chang T-C, Mendell JT, Salzberg SL**.
824 2015. StringTie enables improved reconstruction of a transcriptome from RNA-seq
825 reads. Nature Biotechnology **33**, 290.
826 **Pizarro EA, Hare MD, Mutimura M, Changjun B**. 2013. *Brachiaria* hybrids:
827 potential, forage use and seed yield. Tropical Grasslands-Forrajes Tropicales **1**, 31-
828 35.
829 **Poschenrieder C, Gunsé B, Corrales I, Barceló J**. 2008. A glance into aluminum
830 toxicity and resistance in plants. Science of the Total Environment **400**, 356-368.
831 **Powell S, Forslund K, Szklarczyk D, Trachana K, Roth A, Huerta-Cepas J,**
832 **Gabaldon T, Rattei T, Creevey C, Kuhn M**. 2014. eggNOG v4. 0: nested orthology
833 inference across 3686 organisms. Nucleic Acids Research **42**, D231-D239.
834 **Raman H, Zhang K, Cakir M, Appels R, Garvin DF, Maron LG, Kochian LV,**
835 **Moroni JS, Raman R, Imtiaz M**. 2005. Molecular characterization and mapping of
836 ALMT1, the aluminium-tolerance gene of bread wheat (*Triticum aestivum* L.).
837 Genome **48**, 781-791.
838 **Rao IM, Miles JW, Beebe SE, Horst WJ**. 2016. Root adaptations to soils with low
839 fertility and aluminium toxicity. Annals of Botany **118**, 593-605.
840 **Roselló M, Poschenrieder C, Gunse B, Barceló J, Llugany M**. 2015. Differential
841 activation of genes related to aluminium tolerance in two contrasting rice cultivars.
842 Journal of inorganic biochemistry **152**, 160-166.
843 **Ryan PR, Raman H, Gupta S, Horst WJ, Delhaize E**. 2009. A second mechanism
844 for aluminum resistance in wheat relies on the constitutive efflux of citrate from roots.
845 Plant Physiology **149**, 340-351.
846 **Salgado LR, Lima R, dos Santos BF, Shirakawa KT, de Almeida Vilela M,**
847 **Almeida NF, Pereira RM, Nepomuceno AL, Chiari L**. 2017. *De novo* RNA
848 sequencing and analysis of the transcriptome of signalgrass (*Urochloa decumbens*)
849 roots exposed to aluminum. Plant Growth Regulation **83**, 157-170.
850 **Schmutz J, McClean PE, Mamidi S, Wu GA, Cannon SB, Grimwood J, Jenkins**
851 **J, Shu S, Song Q, Chavarro C**. 2014. A reference genome for common bean and
852 genome-wide analysis of dual domestications. Nature Genetics **46**, 707.

853 **Simão FA, Waterhouse RM, Ioannidis P, Kriventseva EV, Zdobnov EM**. 2015.
854 BUSCO: assessing genome assembly and annotation completeness with single-
855 copy orthologs. Bioinformatics **31**, 3210-3212.
856 **Smit AF, Hubley R**. 2008. RepeatModeler Open-1.0. Available from http://www.
857 repeatmasker. org.
858 **Stanke M, Keller O, Gunduz I, Hayes A, Waack S, Morgenstern B**. 2006.
859 AUGUSTUS: ab initio prediction of alternative transcripts. Nucleic Acids Research
860 **34**, W435-W439.
861 **Tamura K, Stecher G, Peterson D, Filipski A, Kumar S**. 2013. MEGA6: molecular
862 evolutionary genetics analysis version 6.0. Molecular Biology and Evolution **30**,
863 2725-2729.
864 **Tanaka N, Uraguchi S, Kajikawa M, Saito A, Ohmori Y, Fujiwara T**. 2018. A rice
865 PHD-finger protein OsTITANIA, is a growth regulator that functions through elevating
866 expression of transporter genes for multiple metals. The Plant Journal **96**, 997-1006.
867 **Tang Y, Garvin DF, Kochian L, Sorrells M, Carver BF**. 2002. Physiological
868 genetics of aluminum tolerance in the wheat cultivar Atlas 66. Crop Science **42**,
869 1541-1546.
870 **Tarailo-Graovac M, Chen N**. 2009. Using RepeatMasker to identify repetitive
871 elements in genomic sequences. Current Protocols in Bioinformatics **25**, Chapter 4,
872 Unit 4.10.
873 **Torkamaneh D, Laroche J, Bastien M, Abed A, Belzile F**. 2017. Fast-GBS: a new
874 pipeline for the efficient and highly accurate calling of SNPs from genotyping-by-
875 sequencing data. BMC Bioinformatics **18**, 5.
876 **Trapnell C, Roberts A, Goff L, Pertea G, Kim D, Kelley DR, Pimentel H, Salzberg**
877 **SL, Rinn JL, Pachter L**. 2012. Differential gene and transcript expression analysis
878 of RNA-seq experiments with TopHat and Cufflinks. Nature Protocols **7**, 562.
879 **Valle CBd, Savidan YH**. 1996. Genetics, cytogenetics, and reproductive biology of
880 *Brachiaria*. In: Miles, John W; Maass, Brigitte L; Valle, Cacilda Borges do; Kumble,
881 Vrinda (eds.). Brachiaria: Biology, agronomy, and improvement. Centro Internacional
882 de Agricultura Tropical (CIAT), 147-163.
883 **Van der Auwera GA, Carneiro MO, Hartl C, Poplin R, Del Angel G, Levy-**
884 **Moonshine A, Jordan T, Shakir K, Roazen D, Thibault J**. 2013. From FastQ data

885 to high-confidence variant calls: the genome analysis toolkit best practices pipeline.
886 Current Protocols in Bioinformatics **43**, Chapter 11, Unit 11.10.
887 **Van Ooijen J**. 2011. Multipoint maximum likelihood mapping in a full-sib family of an
888 outbreeding species. Genetics Research **93**, 343-349.
889 **Van Ooijen J, Kyazma B**. 2009. MapQTL® 6, Software for the mapping of
890 quantitative trait in experiment populations of diploid species. Kyazma BV,
891 Wageningen.
892 **Venturini L, Caim S, Kaithakottil GG, Mapleson DL, Swarbreck D**. 2018.
893 Leveraging multiple transcriptome assembly methods for improved gene structure
894 annotation. GigaScience **7**, giy093.
895 **Von Uexküll H, Mutert E**. 1995. Global extent, development and economic impact
896 of acid soils. Plant and Soil **171**, 1-15.
897 **Wenzl P, Arango A, Chaves AL, Buitrago ME, Patino GM, Miles J, Rao IM**. 2006.
898 A greenhouse method to screen brachiariagrass genotypes for aluminum resistance
899 and root vigor. Crop Science **46**, 968-973.
900 **Wenzl P, Patino GM, Chaves AL, Mayer JE, Rao IM**. 2001. The high level of
901 aluminum resistance in signalgrass is not associated with known mechanisms of
902 external aluminum detoxification in root apices. Plant Physiology **125**, 1473-1484.
903 **Wickham H, Chang W**. 2008. ggplot2: An implementation of the Grammar of
904 Graphics. R package version 0.7, URL: http://CRAN. R-project. org/package=
905 ggplot2
906 **Worthington M, Heffelfinger C, Bernal D, Quintero C, Zapata YP, Perez JG, De**
907 **Vega J, Miles J, Dellaporta S, Tohme J**. 2016. A parthenogenesis gene candidate
908 and evidence for segmental allopolyploidy in apomictic *Brachiaria decumbens*.
909 Genetics **203**, 1117-1132.
910 **Wu TD, Reeder J, Lawrence M, Becker G, Brauer MJ**. 2016. GMAP and GSNAP
911 for genomic sequence alignment: enhancements to speed, accuracy, and
912 functionality. In: *Statistical Genomics*: Springer, 283-334.
913 **Yamaji N, Huang CF, Nagao S, Yano M, Sato Y, Nagamura Y, Ma JF**. 2009. A
914 zinc finger transcription factor ART1 regulates multiple genes implicated in aluminum
915 tolerance in rice. The Plant Cell **21**, 3339-3349.
916 **Yang JL, Zhu XF, Peng YX, Zheng C, Li GX, Liu Y, Shi YZ, Zheng SJ**. 2011. Cell
917 wall hemicellulose contributes significantly to aluminum adsorption and root growth
918 in *Arabidopsis*. Plant Physiology **155**, 1885-1892.

Yokosho K, Yamaji N, Ma JF. 2011. An Al-inducible MATE gene is involved in external detoxification of Al in rice. The Plant Journal **68**, 1061-1069.

Zhang G, Liu X, Quan Z, Cheng S, Xu X, Pan S, Xie M, Zeng P, Yue Z, Wang W. 2012. Genome sequence of foxtail millet (*Setaria italica*) provides insights into grass evolution and biofuel potential. Nature Biotechnology **30**, 549.

925 **Table 1:** Statistics associated with the assembly of the *Brachiaria ruziziensis*
926 reference genome and anchored in pseudo-molecules.

	Whole genome assembly (WGA)	**Pruned WGA***	**Anchored assembly**
Total length	732.5 Mbp	533.9 Mbp	525.1 Mbp
% Ns	10.6 %	11.7 %	12.18 %
Number sequences	102,579	23,076	7 pseudo-chrs
N50	27.8 Kbp	44.6 Kbp	55.9 Mbp
N20	76.1 Kbp	91.7 Kbp	62.7 Mbp
N80	3.9 Kbp	19.5 Kbp	44.1 Mbp

927 WGA deposited in NCBI, accession number GCA_003016355. Anchoring available in
928 AGP format, together with the raw reads, in the Bioproject PRJNA437375.
929 *Sequences without genes and under 10Kbp have been removed. Ns: Ambiguous
930 nucleotides.

931 **Table 2:** *Brachiaria* genes differentially expressed during Al^{3+} in *Brachiaria* highlighted in our analysis.

GeneID	Bruz	Bdec	Gene name	*P. halli*	*S. itallica*	*S. viridis*	*A. thaliana*	Uniprot	Function and induction
29G2	**0.71**	**0.17**	STOP1	3G044400	7G287100	7G299300	AT1G34370	STOP1_ORYSJ	Zinc-finger Transcription factor involved in aluminium tolerance
61G2	**0.88**	**0.23**	Citrate transporter detoxification 42	9G552400	9G489200	9G493200	AT1G51340	DTX42_ARATH	Citrate transporter responsible for citrate exudation into the rhizosphere to protect roots from aluminium toxicity. Up-regulated by aluminium. Expressed in roots, but not in shoots.
94G8	**7.68**	**2.36**	P transmembrane transporter	7G133200	7G082600	7G090100	AT4G13420	HAK1_ORYSJ	**In the QTL.** Potassium transmembrane transported induced by P starvation exclusively in roots.
126G26	**1.83**	**0.95**	STOP1	6G306100	6G252000	6G256600	AT5G22890	STOP1_ORYSJ	Transcription factor involved in aluminium tolerance
259G14	**2.36**	**1.43**	Citrate transporter protein detox. 42	9G201000	9G204700	9G203100	AT1G51340	DTX42_ARATH	Citrate transporter responsible for citrate exudation into the rhizosphere to protect roots from aluminium toxicity. Up-regulated by aluminium. Expressed in roots, but not in shoots.
462G24	**-2.35**	**0.38**	AMLT10	4G147500	4G162600	4G130000	-	K3XVN8_SETIT	Aluminium-activated malate transporter 10-like
598G8	**-0.97**	**-2.58**	Cytochrome P450	7G003400	1G019400	1G019300	AT5G07990	C93G1_ORYS	**In the QTL.** Metal-binding transmembrane P450 cytochromes
675G12	**4.27**	**3.89**	Citrate transporter protein detox. 42	5G042400	9G489200	9G493200	AT1G51340	DTX42_ARATH	Citrate transporter responsible for citrate exudation into the rhizosphere to protect roots from aluminium toxicity. Up-regulated by aluminium. Expressed in roots, but not in shoots.
869G16	**1.36**	**1.83**	Cysteine XCP1 protease	2G435100	8G204200	8G213900	AT4G35350	XCP1_ARATH	**In the QTL.** A proteinase that may have a developmental senescence specific cell death function during apoptosis and metal detoxification
1615G2	**2.69**	**1.29**	STOP1	6G306100	6G252000	6G256600	AT5G22890	STOP1_ORYSJ	Zinc-finger Transcription factor involved in aluminium tolerance
1984G2	**1.09**	**0.82**	SLK2	4G345700	4G015400	4G015300	AT5G62090	SLK2_ARATH	DNA-binding adapter subunit of the SEU-SLK2 transcriptional corepressor of abiotic stress (e.g. salt and osmotic stress) response genes by facilitating auxin response and sustaining meristematic potential.
2499G8	**1.18**	**-0.15**	OsTITANIA/AtOBE3	9G552000	9G488800	9G492800	AT1G14740	TTA1_ORYSJ	Widely expressed transcription factor that functions as regulator of metal transporter genes responsible for essential metals delivery to shoots and normal plant growth. Required for the maintenance of metal transporter gene expression, such as IRT1, IRT2, ZIP1, ZIP9, NRAMP1 and NRAMP5.
2708G4	**1.64**	**1.94**	Auxin transport protein BIG	2G178200	2G154800	2G160200	AT3G02260	BIG_ORYSJ	Auxin-mediated developmental responses (e.g. cell elongation, apical dominance, lateral root production, inflorescence architecture, general growth and development).
3096G6	**0.51**	**0.27**	ALS1	9G083700	9G088000	9G086400	AT5G39040	AB25B_ORYSJ	Metal transporter involved in the sequestration of aluminium into vacuoles, which is required for cellular detoxification of aluminium. Induced by aluminium in roots. Expressed in primary roots and lateral roots.
3672G6	**2.54**	**2.26**	NRAT1	1G025100	1G098100	1G097200	AT1G80830	NRAT1_ORYSJ	Metal transporter Al3+, but not divalent cations Fe2+, Mg2+, Cd2+. Involved in Al tolerance by taking up Al in root cells, where it is detoxified by chelation with organic acid anions and sequestration into the vacuoles. Induced by aluminium in roots. Positively regulated by ART1.
4534G2	**4.74**	**0.43**	SAD2 importin beta-like transporter	7G101600	7G051600	7G057300	AT2G31660	SAD2_ARATH	Involved in the regulation of the abscisic acid (ABA)-mediated pathway in response to cold or salt stress, UV-B responses. Involved in trichome initiation. Negative regulator miRNA activity. Expressed in roots, epidermal and guard cells of leaves, stems and siliques
5233G2	**1.07**	**1.18**	XTH23	4G029300	4G246200	4G258800	AT4G25810	XTH23_ARATH	Xyloglucan endotransglucosylase hydrolase protein 23 cleaves and religates xyloglucan polymers, an essential constituent of the primary

									cell wall, and thereby participates in cell wall construction of growing tissues. Up-regulated by abscisic acid (ABA).
5400G2	**-1.38**	**-0.05**	XTH	8G197800	8G142000	8G151900	AT5G13870	XTH5_ARATH	Cleaves and religates xyloglucan polymers, an essential constituent of the primary cell wall, and thereby participates in cell wall construction of growing tissues. Strongly down regulated by abscisic acid. Root specific.
6544G2	**-0.07**	**0.95**	XTH32	2G372300	2G313800	2G324800	AT2G36870	XTH8_ORYSJ	Xyloglucan endotransglucosylase hydrolase protein 32 cleaves and religates xyloglucan polymers, an essential constituent of the primary cell wall, and thereby participates in cell wall construction of growing tissues. May be involved in cell elongation processes. Induced by gibberellic acid (GA3).
6944G2	**1.92**	**2.01**	Phospholipid transporting ATPase	4G247400	4G147300	4G165700	AT1G26130	ALA12_ARATH	Involved in transport of phospholipids.
7361G2	**2.26**	**1.39**	STAR2/ALS3	3G099200	3G043600	3G044400	AT2G37330	STAR2_ORYSJ	Associates with STAR2 to form a functional transmembrane ABC transporter required for detoxification of aluminium (Al) in roots. Can specifically transport UDP-glucose. Induced by Al in roots. Positively regulated by ART1. Root specific.
8068G4	**2.77**	**2.12**	Mg transporter MRS2-D	7G150800	7G099600	7G107500	AT3G19640	MRS2D_ORYSJ	Putative magnesium transporter.
8234G4	**-1.40**	**-1.30**	Uncharacterised	-	-	-	-	A0A3L6T2E7_PANMI	**In the QTL.** Uncharacterised protein.
8440G2	**0.88**	**-1.68**	Cytochrome P450	6G227500	2G094000	2G096800	AT4G36380	C90C1_ARATH	**In the QTL.** Metal-binding transmembrane P450 cytochromes
8448G4	**0.59**	**1.26**	STAR1	4G029500	4G246800	4G259400	AT1G67940	STAR1_ORYSJ	Associates with STAR2 to form a functional transmembrane ABC transporter required for detoxification of aluminium (Al) in roots. Can specifically transport UDP-glucose. Induced by Al in roots. Positively regulated by ART1. Root specific.
11634G4	**0.04**	**4.75**	AMLT1	7G143300	7G007400	7G102000	AT3G11680	ALMT8_ARATH	Malate transporter.
11683G4	**1.00**	**0.66**	XTH27	-	-	-	-	A0A1D6K9K3_ZM	Xyloglucan endotransglucosylase hydrolase protein 27 cleaves and religates xyloglucan polymers, an essential constituent of the primary cell wall, and thereby participates in cell wall construction of growing tissues.
12087G2	**1.31**	**3.21**	Phosphate transporter pho1-2	1G440700	1G360400	1G367100	AT3G23430	PHO12_ORYSJ	Involved in the transfer of inorganic phosphate (Pi) from roots to shoots. Not induced by Pi deficiency in roots. Specifically expressed in roots.
26018G2	**1.08**	**0.98**	transporter NRT1 nitrate transporter	9G390400	9G327900	9G333900	AT2G26690	PTR27_ARATH	Low-affinity proton-dependent nitrate transporter. Up-regulated in the shoots by nitrate, but no changes in the roots.
30107G2	**3.24**	**3.02**	NRAT1	2G074500	1G098100	1G097200	AT1G80830	NRAT1_ORYSJ	Metal transporter Al3+, but not divalent cations Fe2+, Mg2+, Cd2+. Involved in Al tolerance by taking up Al in root cells, where it is detoxified by chelation with organic acid anions and sequestration into the vacuoles. Induced by aluminium in roots. Positively regulated by ART1.

GeneID: Gene number in our reference genome. Bruz/Bdec: Differential expression fold-change values in *B. ruziziensis* and *B. decumbens,* significant p-values under 0.05 are coloured. *P. halli/S. itallica/S. viridis/A. thaliana*: Top Blastp result in each of these species. Uniprot and “Function and induction”: Top Blastp result and associated annotation in the Uniprot database.

935 **Figure 1:** Root growth in *B. decumbens* accession CIAT 606 and *B. ruziziensis*
936 accession BRX 44-02 (cv. Basilisk) after growing for 20 days in control and high (200
937 μM) Al^{3+} concentration hydroponic solutions.
938

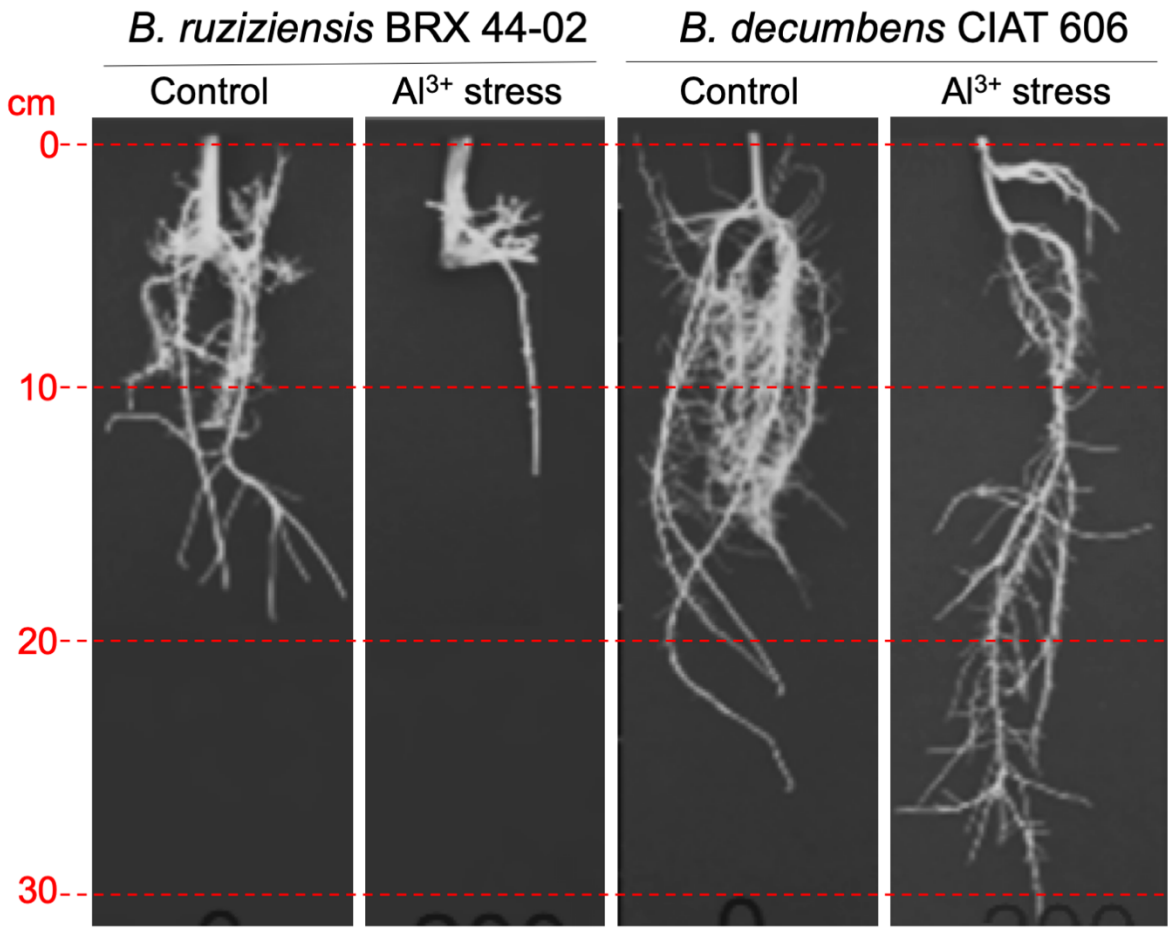

939
940

941 **Figure 2:** Root length (RL), root biomass (RB), and root tip diameter (RD) ratio values
942 between Al^{3+} stress and control measured values (stress/control) in the interspecific
943 progeny (n=169) between *B. ruziziensis* BRX 44-02 and *B. decumbens* CIAT 606 (cv.
944 Basilisk).
945

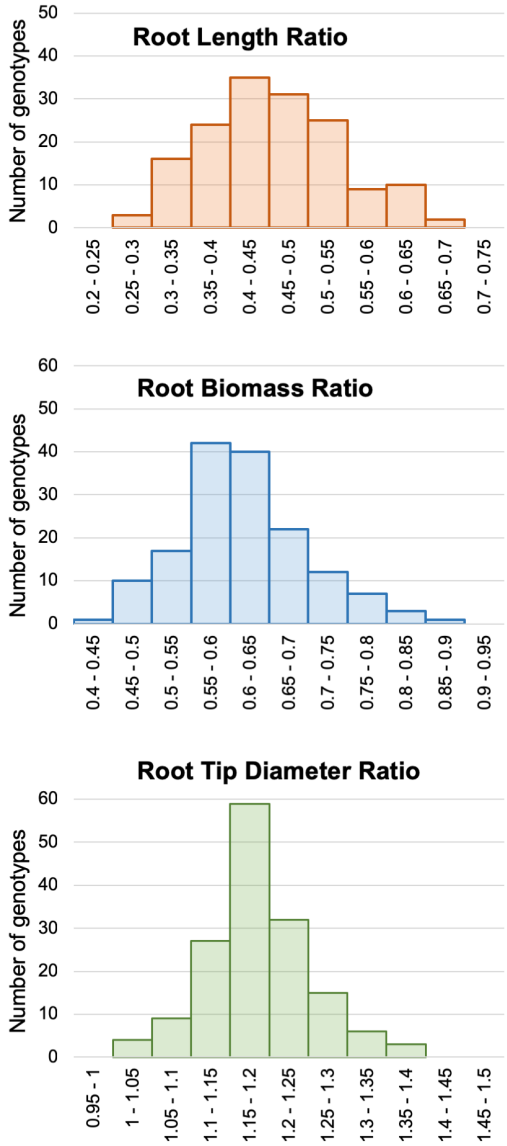

946

Figure 3: Synteny between the *Brachiaria ruziziensis* and foxtail millet (*Setaria italica*) genomes. The 36 synteny blocks longer than 1 Mbp and translocations are highlighted in red or green boxes according to their direction.

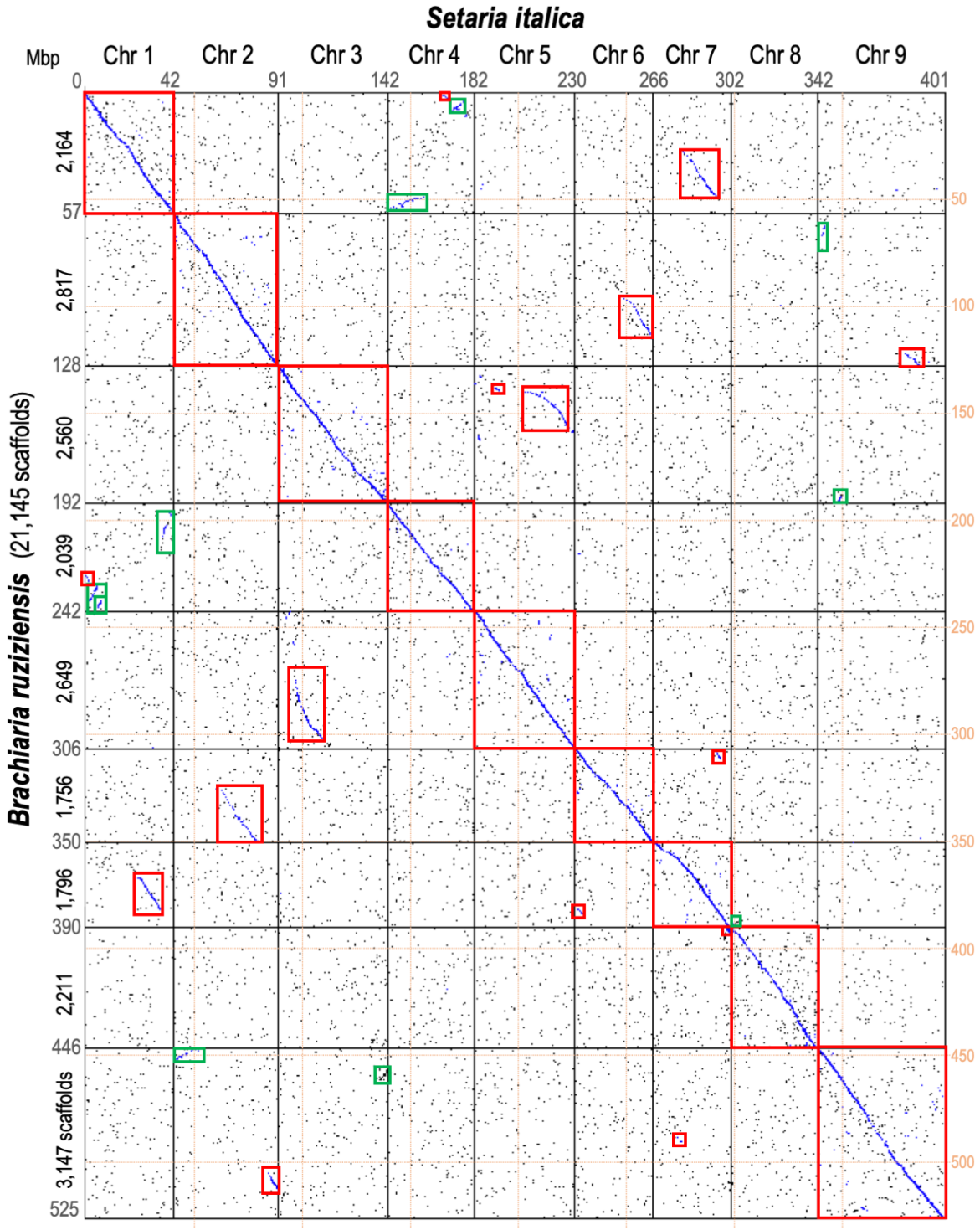

Figure 4: 4,427 genetic markers placed in 18 linkage groups. We defined three QTLs each in LG 1 (Chr 8) for root length and biomass under control and Al^{3+} stress conditions, LG 3 (Chr 7) for root length ratio and root tip diameter ratio (stress/control), and LG 4 (Chr 3) for root tip diameter ratio.

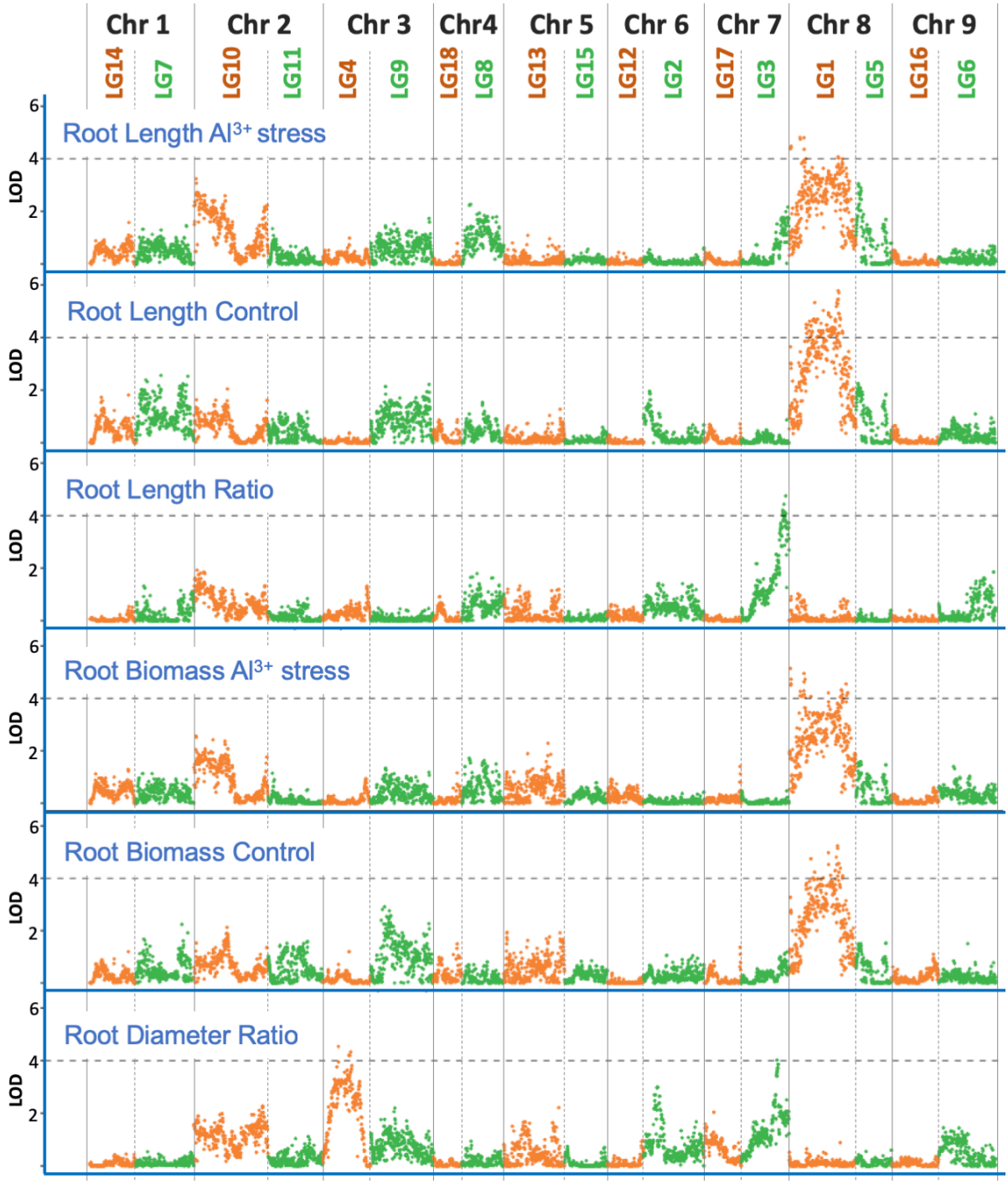

958 **Figure 5:** Differentially expressed (DE) genes in roots and stems from the
959 susceptible genotype *B. ruziziensis* BRX 44-02 and the tolerant genotype *B.*
960 *decumbens* CIAT 606 (cv. Basilisk) between control and high (200 µM $AlCl_3$)
961 aluminium cation concentrations in hydroponic experiments at CIAT.
962

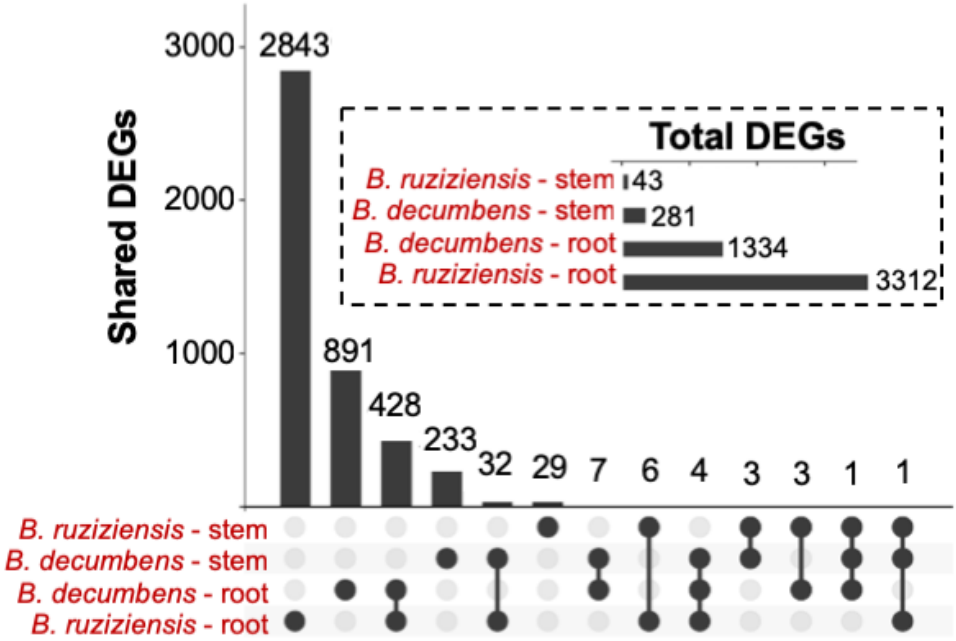

963
964

965 **Figure 6:** Enrichment analysis of the GO slim terms overrepresented among
966 differentially expressed genes that are either up-regulated (red) or down-regulated
967 (blue) during stress in roots from the susceptible *B. ruziziensis* BRX 44-02 (*B.ruziz*)
968 or the tolerant genotype *B. decumbens* CIAT 606 cv. Basilisk (*B.decu*) genotypes.
969

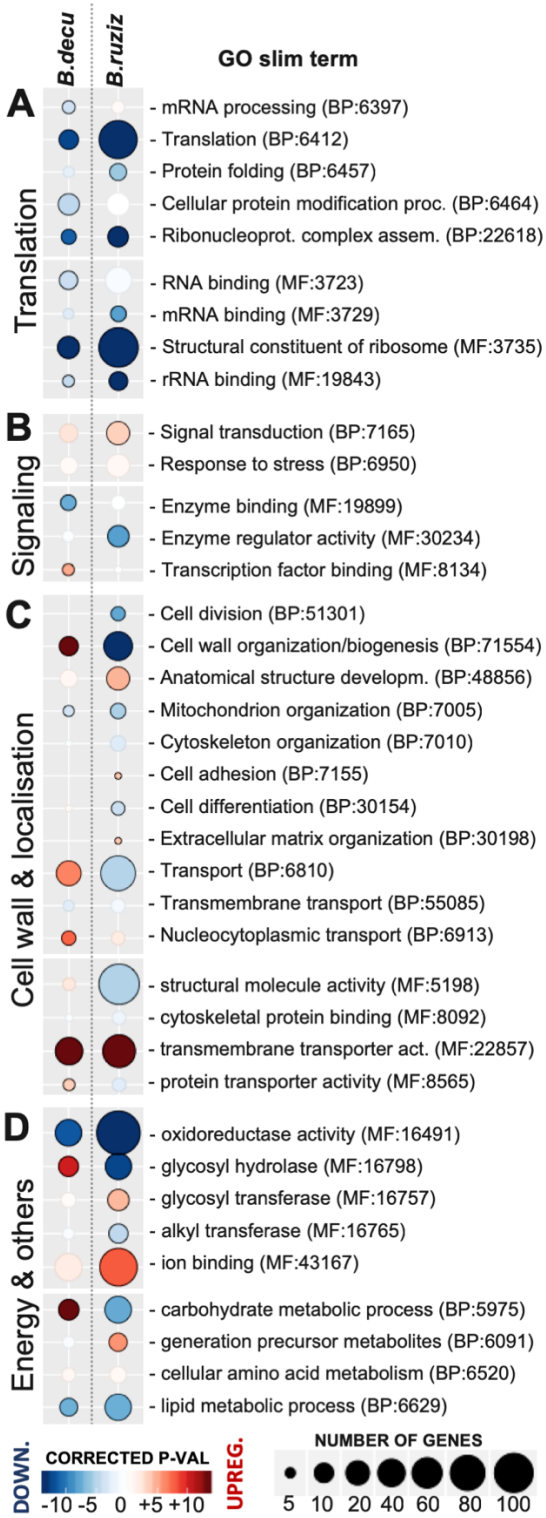

970